Available on CMS information server

CMS NOTE -2023/006

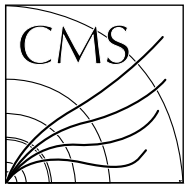

The Compact Muon Solenoid Experiment

CMS Note

Mailing address: CMS CERN, CH-1211 GENEVA 23, Switzerland

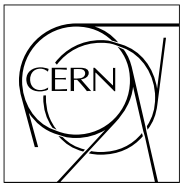

01 July 2023 (v2, 19 July 2023)

Production and validation of industrially produced large-sized GEM foils for the Phase-2 upgrade of the CMS muon spectrometer

M. Abbas, M. Abbrescia, H. Abdalla, A. Abdelalim, S. AbuZeid, D. Aebi, A. Agapitos, A. Ahmad, A. Ahmed, W. Ahmed, C. Aimè, T. Akhter, B. Alsufyani, C. Aruta, I. Asghar, P. Aspell, C. Avila, J. Babbar, Y. Ban, R. Band, S. Bansal, L. Benussi, V. Bhatnagar, M. Bianco, S. Bianco, K. Black, L. Borgonovi, O. Bouhali, A. Braghieri, S. Braibant, S. Butalla, A. Cagnotta, S. Calzaferri, R. Campagnola, M. Caponero, J. Carlson, F. Cassese, N. Cavallo, S.S. Chauhan, B. Choudhary, S. Colafranceschi, A. Colaleo, A. Conde Garcia, A. Datta, A. De Iorio, G. De Lentdecker, D. Dell Olio, G. De Robertis, W. Dharmaratna, T. Elkafrawy, R. Erbacher, P. Everaerts, F. Fabozzi, F. Fallavollita, D. Fiorina, M. Franco, C. Galloni, P. Giacomelli, S. Gigli, J. Gilmore, M. Gola, A. Gutierrez, R. Hadjiiska, K. Hoepfner, M. Hohlmann, Y. Hong, H. Hoorani, T. Huang, P. Iaydjiev, A. Irshad, A. Iorio, F. Ivone, W. Jang, J. Jaramillo, Y. Jeong, Y. Jeng, E. Juska, B. Kailasapathy, T. Kamon, Y. Kang, P. Karchin, A. Kaur, H. Kaur, H. Keller, H. Kim, J. Kim, S. Kim, B. Ko, A. Kumar, S. Kumar, N. Lacalamita, J.S.H. Lee, A. Levin, Q. Li, F. Licciulli, L. Lista, K. Liyanage, F. Loddo, M. Luhach, M. Maggi, Y. Maghrbi, N. Majumdar, K. Malagalage, S. Martiradonna, C. McLean, J. Merlin, M. Misheva, G. Mocellin, L. Moureaux, A. Muhammad, S. Muhammad, S. Mukhopadhyay, M. Naimuddin, S. Nuzzo, R. Oliveira, P. Paolucci, I.C. Park, L. Passamonti, G. Passeggio, A. Peck, A. Pellecchia, N. Perera, L. Petre, D. Piccolo, D. Pierluigi, G. Raffone, F. Ramirez, A. Ranieri, G. Rashevski, D. Rathjens, B. Regnery, C. Rendon, C. Riccardi, B. Rossi, P. Rout, J. D. Ruiz, A. Russo, A. Safonov, A. K. Sahota, D. Saltzberg, G. Saviano, A. Shah, A. Sharma, R. Sharma, T. Sheokand, M. Shopova, F. Simone, J. Singh, U. Sonnadara, J. Sturdy, G. Sultanov, Z. Szillasi, D. Teague, D. Teyssier, M. Tytgat, I. Vai, N. Vanegas, R. Venditti, P. Verwilligen, W. Vetens, A.K. Virdi, P. Vitulo, A. Wajid, D. Wang, K. Wang, I.J. Watson, N. Wickramage, D.D.C. Wickramarathna, E. Yanes, S. Yang, U. Yang, Y. Yang, I. Yoon, Z. You, I. Yu, S. Zaleski,

Abstract

The upgrade of the CMS detector for the high luminosity LHC (HL-LHC) will include gas electron multiplier (GEM) detectors in the end-cap muon spectrometer. Due to the limited supply of large area GEM detectors, the Korean CMS (KCMS) collaboration had formed a consortium with Mecaro Co., Ltd. to serve as a supplier of GEM foils with area of approximately 0.6 m^2. The consortium has developed a double-mask etching technique for production of these large-sized GEM foils. This article describes the production, quality control, and quality assessment (QA/QC) procedures and the mass production status for the GEM foils. Validation procedures indicate that the structure of the Korean foils are in the designed range. Detectors employing the Korean foils satisfy the requirements of the HL-LHC in terms of the effective gain, response uniformity, rate capability, discharge probability, and hardness against discharges. No aging phenomena were observed with a charge collection of 82 mC/cm^2. Mass production of KCMS GEM foils is currently in progress.

Production and validation of industrially produced large-sized GEM foils for the Phase-2 upgrade of the CMS muon spectrometer

M. Abbas[n], M. Abbrescia[s], H. Abdalla[i,k], A. Abdelalim[i,l], S. AbuZeid[j,w], D. Aebi[ag], A. Agapitos[e], A. Ahmad[ac], A. Ahmed[q], W. Ahmed[ac], C. Aimè[w], T. Akhter[ag], B. Alsufyani[al], C. Aruta[s,1], I. Asghar[ac], P. Aspell[af], C. Avila[g], J. Babbar[p], Y. Ban[e], R. Band[ai,2], S. Bansal[p], L. Benussi[u], V. Bhatnagar[p], M. Bianco[af], S. Bianco[u], K. Black[ak], L. Borgonovi[t], O. Bouhali[ag], A. Braghieri[w], S. Braibant[t], S. Butalla[al], A. Cagnotta[v], S. Calzaferri[w], R. Campagnola[u], M. Caponero[u], J. Carlson[ah], F. Cassese[v], N. Cavallo[v], S.S. Chauhan[p], B. Choudhary[q], S. Colafranceschi[u], A. Colaleo[s], A. Conde Garcia[af], A. Datta[ah], A. De Iorio[v], G. De Lentdecker[a], D. Dell Olio[s], G. De Robertis[s], W. Dharmaratna[ae], T. Elkafrawy[al], R. Erbacher[ai], P. Everaerts[ak], F. Fabozzi[v], F. Fallavollita[af,3], D. Fiorina[w], M. Franco[s], C. Galloni[ak], P. Giacomelli[t], S. Gigli[w], J. Gilmore[ag], M. Gola[q], A. Gutierrez[aj], R. Hadjiiska[d], K. Hoepfner[m], M. Hohlmann[al], Y. Hong[c], H. Hoorani[ac], T. Huang[ag], P. Iaydjiev[d], A. Irshad[a], A. Iorio[v], F. Ivone[m], W. Jang[aa], J. Jaramillo[h], Y. Jeong[z,4], Y. Jeng[x], E. Juska[ag], B. Kailasapathy[ad,ae], T. Kamon[ag], Y. Kang[aa], P. Karchin[aj], A. Kaur[p], H. Kaur[q], H. Keller[m], H. Kim[ag], J. Kim[y], S. Kim[aa], B. Ko[aa], A. Kumar[q], S. Kumar[p], N. Lacalamita[s], J.S.H. Lee[aa], A. Levin[e], Q. Li[e], F. Licciulli[s], L. Lista[v], K. Liyanage[ae], F. Loddo[s], M. Luhach[p], M. Maggi[s], Y. Maghrbi[ab], N. Majumdar[r], K. Malagalage[ad], S. Martiradonna[s], C. McLean[ai,5], J. Merlin[x], M. Misheva[d], G. Mocellin[ai], L. Moureaux[a], A. Muhammad[ac], S. Muhammad[ac], S. Mukhopadhyay[r], M. Naimuddin[q], S. Nuzzo[s], R. Oliveira[af], P. Paolucci[v], I.C. Park[aa], L. Passamonti[u], G. Passeggio[v], A. Peck[aj,6], A. Pellecchia[s], N. Perera[ae], L. Petre[a], D. Piccolo[u], D. Pierluigi[u], G. Raffone[u], F. Ramirez[h], A. Ranieri[s], G. Rashevski[d], D. Rathjens[ag], B. Regnery[ai,7], C. Rendon[c], C. Riccardi[w], B. Rossi[v], P. Rout[r], J. D. Ruiz[h], A. Russo[u], A. Safonov[ag], A. K. Sahota[p], D. Saltzberg[ah], G. Saviano[u], A. Shah[q], A. Sharma[af], R. Sharma[q], T. Sheokand[p], M. Shopova[d], F. Simone[s], J. Singh[p], U. Sonnadara[ad], J. Sturdy[aj], G. Sultanov[d], Z. Szillasi[o], D. Teague[ak], D. Teyssier[o], M. Tytgat[b,c], I. Vai[w], N. Vanegas[h], R. Venditti[s], P. Verwilligen[s], W. Vetens[ak], A.K. Virdi[p], P. Vitulo[w], A. Wajid[ac], D. Wang[e], K. Wang[e],

[*]Corresponding author.

[1]Present address: University of Florida, Gainesville, USA

[2]Present address: University of Notre Dame, Notre Dame, USA

[3]Present address: Max Planck Institut für Physik, München, Germany

[4]Present address: Korea Astronomy and Space Science Institute, Daejeon, Republic of Korea

[5]Present address: Argonne National Laboratory, Lemont, USA

[6]Present address: Boston University, Boston, USA

[7]Present address: Karlsruhe Institute of Technology, Karlsruhe, Germany

I.J. Watson[aa], N. Wickramage[ae], D.D.C. Wickramarathna[ad], E. Yanes[al], S. Yang[aa], U. Yang[y], Y. Yang[a], I. Yoon[y,*], Z. You[f], I. Yu[z], S. Zaleski[m]

[a] *Université Libre de Bruxelles, Bruxelles, Belgium*
[b] *Vrije Universiteit Brussel, Brussels, Belgium*
[c] *Ghent University, Ghent, Belgium*
[d] *Institute for Nuclear Research and Nuclear Energy, Bulgarian Academy of Sciences, Sofia, Bulgaria*
[e] *Peking University, Beijing, China*
[f] *Sun Yat-Sen University, Guangzhou, China*
[g] *University de Los Andes, Bogota, Colombia*
[h] *Universidad de Antioquia, Medellin, Colombia*
[i] *Academy of Scientific Research and Technology - ENHEP, Cairo, Egypt*
[j] *Ain Shams University, Cairo, Egypt*
[k] *Cairo University, Cairo, Egypt*
[l] *Helwan University, also at Zewail City of Science and Technology, Cairo, Egypt*
[m] *RWTH Aachen University, III. Physikalisches Institut A, Aachen, Germany*
[n] *Karlsruhe Institute of Technology, Karlsruhe, Germany*
[o] *Institute for Nuclear Research ATOMKI, Debrecen, Hungary*
[p] *Panjab University, Chandigarh, India*
[q] *Delhi University, Delhi, India*
[r] *Saha Institute of Nuclear Physics, Kolkata, India*
[s] *Politecnico di Bari, Università di Bari and INFN Sezione di Bari, Bari, Italy*
[t] *Università di Bologna and INFN Sezione di Bologna, Bologna, Italy*
[u] *Laboratori Nazionali di Frascati INFN, Frascati, Italy*
[v] *Università di Napoli and INFN Sezione di Napoli, Napoli, Italy*
[w] *Università di Pavia and INFN Sezione di Pavia, Pavia, Italy*
[x] *Hanyang University, Seoul, Korea*
[y] *Seoul National University, Seoul, Korea*
[z] *Sungkyunkwan University, Gyeonggi, Republic of Korea*
[aa] *University of Seoul, Seoul, Korea*
[ab] *College of Engineering and Technology, American University of the Middle East, Dasman, Kuwait*
[ac] *National Center for Physics, Islamabad, Pakistan*
[ad] *University of Colombo, Colombo, Sri Lanka*
[ae] *University of Ruhuna, Matara, Sri Lanka*
[af] *CERN, Geneva, Switzerland*
[ag] *Texas A&M University, College Station, USA*
[ah] *University of California, Los Angeles, USA*
[ai] *University of California, Davis, USA*
[aj] *Wayne State University, Detroit, USA*
[ak] *University of Wisconsin, Madison, USA*
[al] *Florida Institute of Technology, Melbourne, USA*

Abstract

The upgrade of the CMS detector for the high luminosity LHC (HL-LHC) will include gas electron multiplier (GEM) detectors in the end-cap muon spectrometer. Due to the limited supply of large area GEM detectors, the Korean CMS (KCMS) collaboration had formed a consortium with Mecaro Co., Ltd. to serve as a supplier of GEM foils with area of approximately $0.6\,\mathrm{m}^2$. The consortium

has developed a double-mask etching technique for production of these large-sized GEM foils. This article describes the production, quality control, and quality assessment (QA/QC) procedures and the mass production status for the GEM foils. Validation procedures indicate that the structure of the Korean foils are in the designed range. Detectors employing the Korean foils satisfy the requirements of the HL-LHC in terms of the effective gain, response uniformity, rate capability, discharge probability, and hardness against discharges. No aging phenomena were observed with a charge collection of $82\,\mathrm{mC\,cm^{-2}}$. Mass production of KCMS GEM foils is currently in progress.

Keywords: GEM, Double-mask, CMS, High luminosity LHC

1. Introduction

Since the concept of a gas electron multiplier (GEM) was introduced [1], the technology has garnered considerable attention from the experimental particle and nuclear physics communities. Owing to its substantially high flux capability, significant hardness to radiation, and high position resolution, GEM technology has been widely applied and adopted for next generation tracking devices in several experiments, including the CMS experiment.

To take advantage of the increased luminosity of the HL-LHC compared to that of the LHC [2], upgrades of the CMS experiment are planned to enhance performance under HL-LHC operating conditions. The upgrades include three stations of GEM detectors for the endcap muon system [3, 5]. These stations, in order of their distance from the interaction point, are called ME0, GE1/1, and GE2/1. The installation of the GE1/1 stations is complete and commissioning is ongoing. Production and assembly of GE2/1 detectors has just begun and will be followed by production for ME0. The GE2/1 (ME0) stations are scheduled to be installed during the LHC year end technical stops 2023-2024, and 2024-2025 (LHC long shutdown 3, 2026-2028) [4, 6].

The GE1/1 station is comprised of two types of detector modules, long and short, to accommodate existing support structures while maximizing acceptance. A short-type module was used for the study presented here. To cover a large area with uniform detector properties, the GE2/1 detectors are comprised of eight modules, labeled M1 to M8. An M7-type module was used for the aging study described at the end of subsection 3.3.

The Korean CMS group (KCMS) is designated as a second supplier of large-sized GEM foils for the CMS upgrades. For a long time, the CERN micro pattern technologies (MPT) workshop was the sole supplier of large-sized GEM foils. This motivated the CMS experiment to find a second supplier of large-sized GEM foils in the industrial sector. For this purpose, the KCMS had formed a consortium with MECARO Co., Ltd., a Korean company producing components and materials for semiconductor production [7]. The objective of the consortium was to contribute to the CMS upgrade, as well as other experiments, by supplying large-sized GEM foils. Korean GEM foils will be produced for and deployed in the GE2/1 and ME0 detectors.

2. GEM foil production

GEM foils are made from flexible copper-clad laminate (FCCL) consisting of 50 µm thick polyimide (PI) coated on both sides with 3–5 µm thick Cu. The foils are perforated by symmetric bi-conical holes with diameter 70 ± 5 µm (Cu) and 55 ± 5 µm (PI). The holes are separated with a pitch of 140 µm.

The consortium is the world's first and sole producer of large-sized GEM foils using a double-mask technique. This technique, employing semi-automated machinery, is significantly simpler and faster than the previously used single-mask technique [8].

With the double-mask technique, the alignment of the top and bottom masks is crucial in producing GEM foils with the proper geometry. The permissible misalignment is less than 7 µm. Fig. 1 presents the large-sized bipolar ultra-violet (UV) exposure machine that aligns the masks through which UV light is irradiated onto dry film photoresist (DFR) laminated on both sides of the FCCL. The misalignment was verified to be approximately 5 µm.

The size of the machine becomes the limiting factor of the size of GEM foils producible. The maximum area exposed to UV radiation and the available area for pattern development is approximately 125×58 cm^2. Emulsion glass masks is adopted for the alignment.

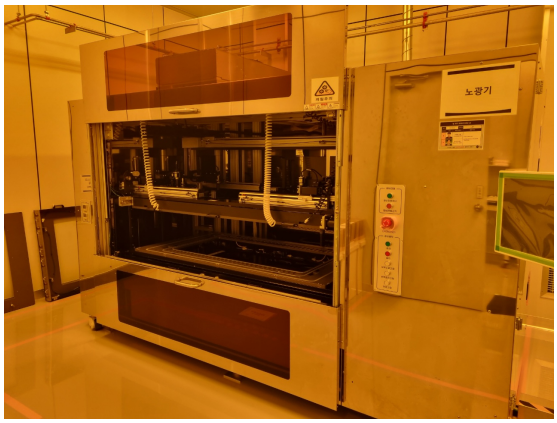

Figure 1: Large-sized bipolar UV exposure machine that aligns top and bottom masks and irradiates UV light to dry film photoresist through the masks.

After the pattern is developed on DFRs, Cu holes are produced via chemical wet etching. The diameter of the holes is tunable by adjusting the etching conditions. The DFR development and Cu etching are carried out by automated conveying machinery. PI holes are manually developed by immersing FCCLs in a bath filled with etchant. Cu layers laminated on the PI layer function as masks for the PI etching processes. A mixture of mono ethanolamine (MEA) and potassium hydroxide is used as the PI etchant [9]. By adjusting the composition of the PI etchant, the geometry of developed PI holes is tunable. To form the supporting areas, such as electrodes, a secondary Cu etching is carried out. For

this etching, emulsion glass masks are not necessary because the alignment of masks is not critical for the support areas. After the post processes, such as resistor soldering, the production is complete.

3. Quality validation

After fabrication, the GE1/1 short-type GEM foils were validated. Fig. 2 shows a GE1/1 foil used for the validation. The GE1/1 foils are single-segmented foils: only the Cu layer facing the drift electrode (drift side) is segmented to control the amount of energy released when a discharge occurs. The opposite layer, facing the readout electrodes (RO side), is not segmented. The GEM detector assembly facility and the CERN gamma irradiation facility++ (GIF++) [10] were utilized for the validation.

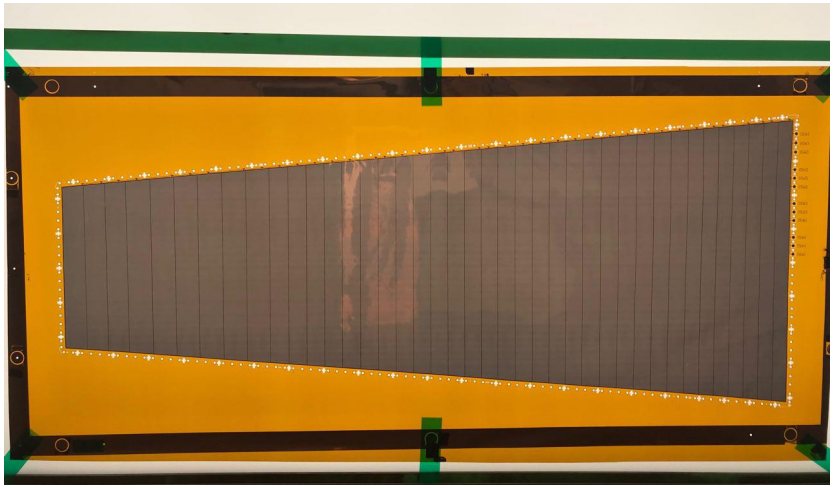

Figure 2: CMS GE1/1 short-type GEM foil fabricated by the KCMS and Mecaro consortium for quality validation. The active area has dimensions 106.1 cm (height) and 23.1–42.0 cm (bases).

3.1. Optical inspection

First, optical inspections were performed to determine the quality of the hole development. Because the properties of the GEM foils depend significantly on the hole geometry, it is important to verify that the etching process produced holes that match the design.

Scanning electron microscope (SEM) images were taken to evaluate the quality of the hole development. Fig. 3 shows SEM images of the drift and readout sides and cross-section of a fabricated GEM foil.

The diameters of the holes were first measured with a manually controlled optical microscope that was calibrated with circular patterns of precise diameters. For 15 positions on the GEM foil and 30 holes for each position, the

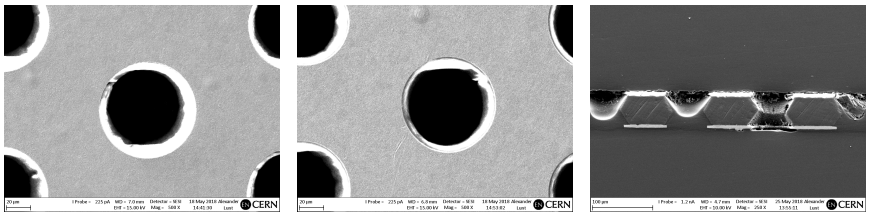

(a) Drift side (b) Readout side (c) Cross section

Figure 3: SEM images of a GEM foil fabricated by Mecaro. In the cross-section view (c), the material visible inside the holes is resin that was added to protect the foil during the cutting and polishing process.

diameters of 450 holes were measured. The Cu (PI) diameters were 70.7 ± 2.0 (50.7 ± 2.0) µm. No significant difference in the diameters was observed based on position. The measurement precision was limited by the microscope.

Since deviation of hole diameter depending on position within a foil is an important factor in uniformity of detector response, an automated 2-D CCD camera scanner [11] is employed to measure the diameter of every hole in a foil. The distribution of deviation in hole diameter is shown in Fig. 4. The distribution is well described by a single Gaussian with variance of the Cu (PI) diameter of 3.08 (2.49) µm. No significant difference in the variance of hole diameters was observed between the drift side and the readout side, showing the successful application of the double-mask technique.

However, it was observed that the diameters of PI holes varied by production batches. Review of the PI etching process pointed to the denaturing of the etchant under reaction with carbon dioxide in air, which was not considered previously. The process was modified so that the etchant is tuned before use with each PI batch. In addition, a strict quality control (QC) protocol is applied. The diameters of Cu holes are observed to be robust.

3.2. Long-term measurement of leakage current and applied voltage in dry nitrogen

After optical inspection of a foil, its leakage current was measured to assess its cleanliness. Because contaminants on the foil can provide electrical bridges between the Cu layers, the foil's impedance is a measure of its cleanliness. It is also important to identify defects in the structure of the foil that may induce sparks. In principle this could be accomplished by optical inspection. However, owing to the microscopic nature of the foil, optical inspection is impractical because it takes a long time and can even be destructive in some cases. Instead, defects can be identified during leakage current measurement by trips of the power supply due to an abrupt increase in current. Thus, measurement of leakage current and trips in applied voltage are practical tools to evaluate the cleanliness and quality of GEM foils.

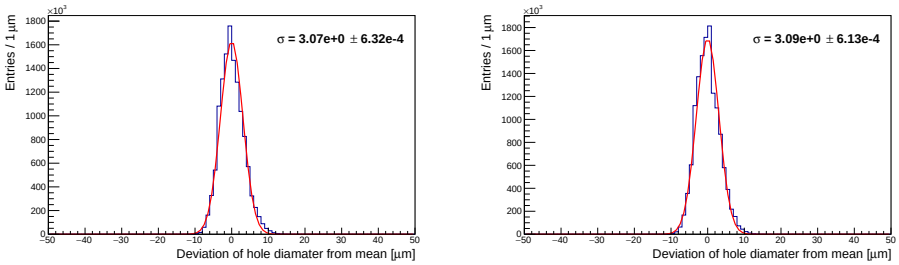

(a) Cu hole, drift side

(b) Cu hole, RO side

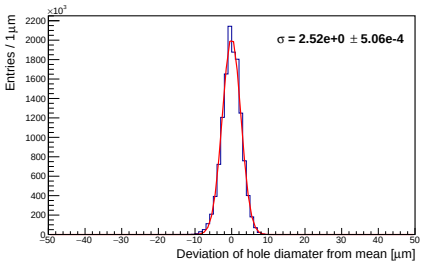

(c) PI hole, drift side

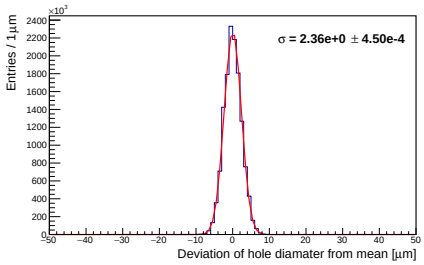

(d) PI hole, RO side

Figure 4: Distributions of deviation of hole diameters from the mean. The first (second) row presents the deviation of Cu (polyimide) hole diameters, while the first (second) column illustrates the deviation measured from the drift (readout) side of the GEM foil. [12].

Leakage current and frequency of discharges were measured with high voltage applied to the GEM foils using a QC methodology developed for the CMS GEM upgrade [13]. The QC procedure consists of two parts, called QC-fast and QC-long. The differences between QC-fast and QC-long are the time duration and atmospheric environment.

The QC-fast is a short test and is performed in ordinary air. Preliminary assessment of a foil is obtained via the QC-fast. The QC-long lasts for at least 7 h, depending on the cleanliness quality of the GEM foils. The QC-long is performed inside a plexiglass container filled with dry nitrogen to control relative humidity.

Fig. 5 presents an example of a QC-long result showing stable, low leakage current without discharge. (No power supply trips were recorded.) Only foils that pass the QC-long test are used in assembling detectors. If a foil shows leakage current more than 5 nA or discharges that occur too frequently, the foil is repeatedly cleaned chemically and physically.

3.3. Quality validation with CMS GE1/1 short-type detectors

Korean GEM foils that passed the QC-long test were used to assemble four CMS GE1/1 short-type detectors. The design of the GE1/1 detectors, which operate with an Ar/CO_2 (70 %/30 %) mixture, is described in detail in [3]. High

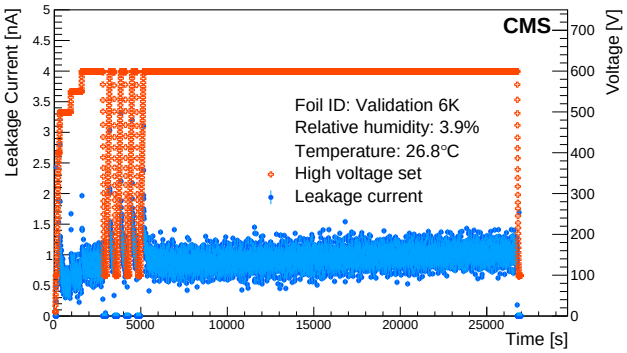

Figure 5: Conventional example of QC-long test result of GEM foil fabricated by KCMS and Mecaro. The horizontal axis represents duration of the test. Applied high voltage to the GEM foil is shown by the red markers. Blue markers denote leakage current. The rapid changes in applied voltage at the beginning of the test are intended to stress the foils.

voltage is supplied using an in-house designed voltage divider. The properties of the detectors were measured to validate the quality of the Korean GEM foils. After assembly, gas tightness and high voltage tests were performed to verify the integrity of the assembly before measurement of key chamber properties, following the procedures described in [14].

Effective Gain: Effective gain (G) is a basic property of a GEM detector and can be used to compare detectors assembled with Mecaro foils with those assembled with CERN foils. The effective gain was calculated from the readout current (I_{ro}) and event rate (R) of detectors irradiated with x-rays from an Amptek Mini-X2 generator with an Ag transmission target. I_{RO} was measured using a Keithley 6487 picoammeter. The effective gain was calculated as $G = \frac{I_{RO}}{R \times q_{el} \times N_p}$, where q_{el} is the electron charge and N_p is the number of primary electrons produced by the photo-electron originating from fluorescence of a copper atom in the drift electrode that has absorbed an x-ray from the generator. N_p is estimated as 346.0 ± 2.9 by comparing the response of a detector to x-rays from the generator with the response to x-rays from ^{55}Fe, as described in [14].

Measurements of effective gain versus high voltage divider current for four detectors are presented in Fig. 6. The divider current is proportional to the high voltage applied to the foils. A current of 660 µA provides a reference working point that can be used to compare the effective gas gain of different detectors. For the four detectors with Mecaro foils, the effective gains were measured to be in the range 5.3×10^3 to 1.2×10^4, consistent with the gains of detectors with CERN foils [14].

Response uniformity: It is important that the signal response from strips in all regions of the detector is uniform to ensure good trigger and track reconstruction efficiencies over the geometrical acceptance of the detector. To measure the response uniformity, as described in detail in [14], detectors were divided into 768 sectors, each sector comprising four readout strips. For each

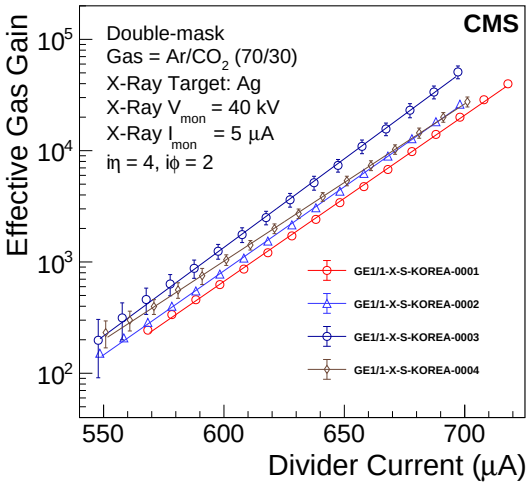

Figure 6: Effective gain versus HV divider current for four CMS GE1/1 short-type detectors assembled with Mecaro foils.

sector, the spectrum of charge was obtained while the detectors were exposed to x-rays. The detector strips were read out by APV25 front-end ASICs [15] and ADCs . The ADC spectrum for each sector was fit with a Cauchy distribution function and a fifth order polynomial to determine the ADC value of the Cu fluorescence peak. The distribution of sector peak ADC values for each of the four detectors with Mecaro foils is shown in Fig. 7. The distributions were fit with a Gaussian function to obtain mean (μ) and variance (σ). Response uniformity, σ/μ, of the four detectors are in the range 10.2 % to 16.2 %, consistent with the uniformities of detectors with CERN foils [14].

Rate capability: To estimate the rate capability of GEM detectors with Mecaro foils, the effective gas gain of the detector was measured as a function of x-ray flux. The gain was measured as discussed previously. X-ray flux was tuned by varying the current of the x-ray tube and the number of Cu attenuators. To control the area of x-ray exposure, a brass collimator with a 2 mm diameter aperture was used. Fast preamplifier electronics were utilized to avoid pileup of the signals. No pileup was observed up to a signal rate of 5×10^5 Hz as determined by the linearity of signal rate versus x-ray tube current. Above that value, the signal rate was estimated via extrapolation based on the linear relationship between the x-ray flux and x-ray tube current, and the effect of the Cu attenuators.

The normalized gas gain versus x-ray flux for a CMS GE1/1 short-type detector assembled with Mecaro foils is shown in Fig. 8. The gain is stable for x-ray fluxes up to 1×10^5 Hz mm^{-2}. The gain drop above that flux is due to the effect of protection resistors in the HV circuit. The GE1/1 chambers are equipped with 10 MΩ surface mounted resistors through which high voltage

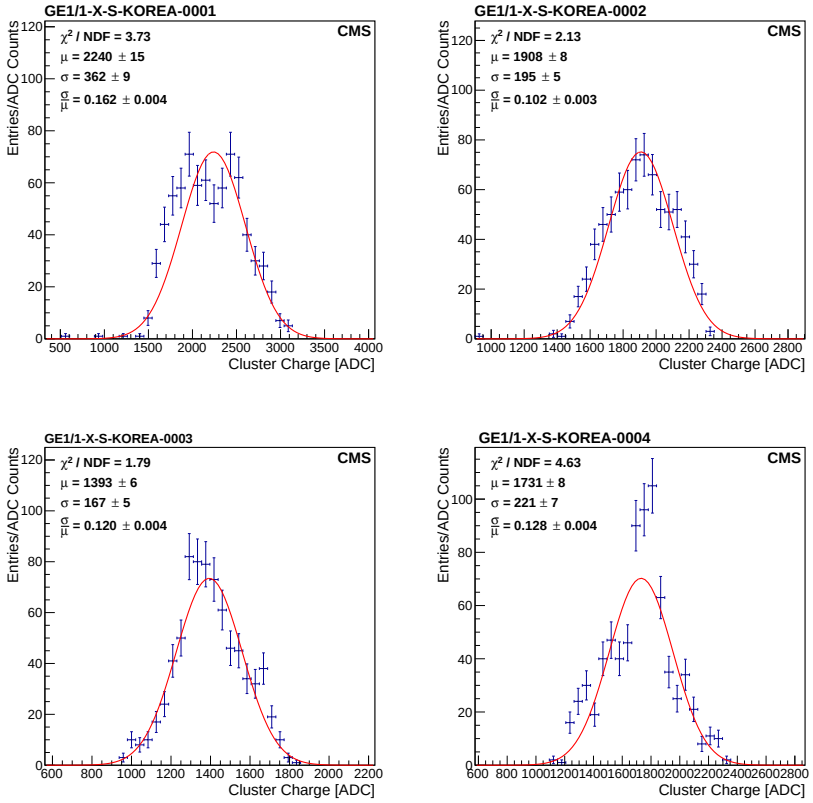

Figure 7: Peak ADC distributions of CMS GE1/1 short-type detectors with Mecaro foils. σ/μ represents the response uniformity of a detector. The response uniformities of the four detectors lie in the range 10.2 % to 16.2 %, consistent with the uniformities of detectors with CERN foils.

is applied to active areas of the GEM foils. When the detectors are exposed to very high x-ray flux, the current flowing through the GEM foils becomes significant, thereby inducing voltage drops across the resistors and reducing the voltage applied to the GEM foils. To verify this behavior, detectors with 10×10 cm^2 GEM foils, fabricated in the same way as larger-sized GE1/1 foils, were equipped with small protection resistors. The flux capability measurement showed the expected increase in normalized gain at high fluxes. The GE1/1 detector with Mecaro foils has comparable flux capability as those fabricated with CERN foils.

Because particle flux varies rapidly with angle from the collision axis, the foils of the ME0 detectors will be radially segmented to equalize the gain drops in the high voltage sectors [16].

Discharge probability and robustness after discharge: Because dis-

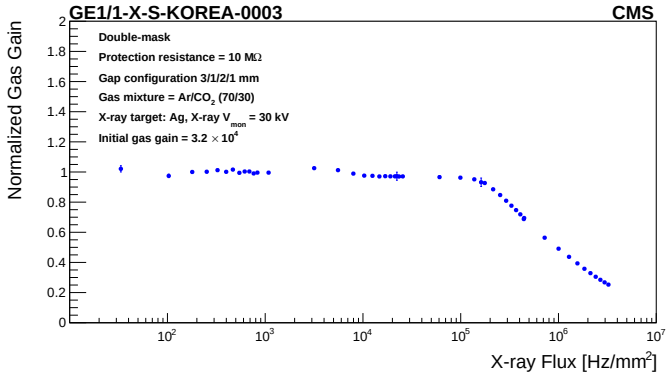

Figure 8: Normalized gas gain versus x-ray flux for a CMS GE1/1 short-type detector assembled with Mecaro foils. The gain remains stable for x-ray fluxes up to $1 \times 10^5\,\mathrm{Hz\,mm^{-2}}$.

charges may damage the GEM foil or readout electronics, the discharge probability should be minimized. Since imperfections in the structure of holes in the GEM foil might induce discharges, it is important to verify that a detector with Korean foils exhibits a discharge probability as low as those of detectors with CERN foils.

Discharges were induced by 5.5 MeV α-particles from ^{241}Am that entered the detector through 5 mm diameter holes drilled into the drift plate. The holes were covered by plastic to prevent gas from leaking. Discharges were detected by the current pulse induced in a wire loop surrounding the high voltage line. To increase the frequency of discharges, the gain was set above the value used in normal operation. The discharge probability at normal gain was estimated by extrapolation.

Fig. 9 presents the measured discharge probability per incident alpha particle, $\frac{N_{discharge}}{N_\alpha}$, as a function of effective gas gain for a GE1/1 short-type detector with Mecaro foils. N_α was measured by the number of current pulses from the GEM readout strips. The uncertainties shown by vertical bars are calculated by the Feldman-Cousins approach [17]. The data were fit with an exponential function using Poisson maximum likelihood. At the reference gain of 1×10^4, the discharge probability is $2.6^{+1.1}_{-0.8} \times 10^{-9}$, consistent with that of detectors with CERN foils [3].

To assess the robustness of the GEM foils to discharges, effective gas gain and energy resolution were compared before and after operation with discharges. There were 229 discharges, most of which occurred at the highest gains. The measurement method for effective gas gain was discussed previously with examples shown in Fig. 6. Measurements of gain versus HV divider current for the same detector before and after operation with discharges are shown in Fig. 10. There is no degradation in gain.

The energy resolution was determined using the 5.9 keV X-ray produced with a ^{55}Fe source. The energy spectra, shown in Fig. 11, were fit with two

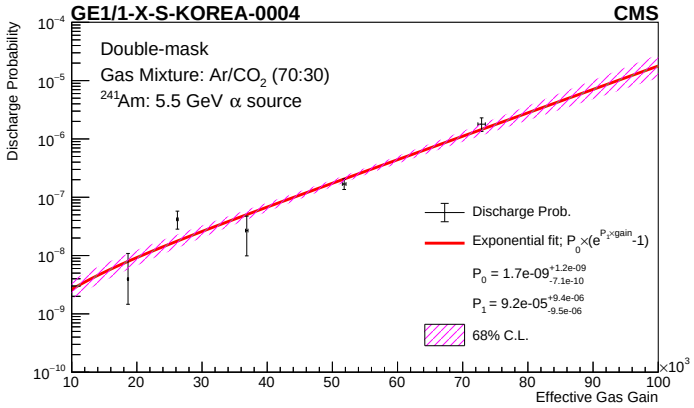

Figure 9: Discharge probability per incident alpha particle and its 68% confidence interval as a function of effective gas gain for of a GE1/1 short-type detector assembled with Mecaro foils. The discharges were induced by 5.5 MeV α-particles from ^{241}Am.

Gaussian functions and a 5th order polynomial to obtain the full width at half maximum of the main peak. The width did not increase after operation with discharges.

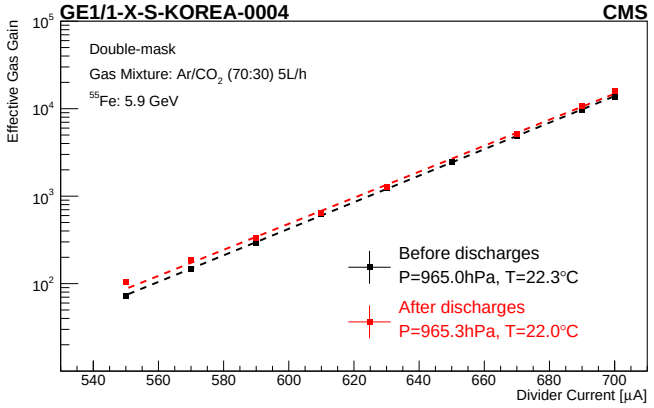

Figure 10: Gain versus HV divider current for a GE1/1 detector with Mecaro foils before and after operation with discharges.

Aging phenomena: The well-established robustness of GEM detectors against classical aging [18] is important for long-term, reliable operation in the harsh HL-LHC environment. At the time of the studies reported here, the background flux for an ME0 detector was expected to result in an accumulated charge of 283 mC cm^{-2} over ten years of operation. The current estimate of the accumulated charge is about thirty times as large and the ME0 HV sectorization

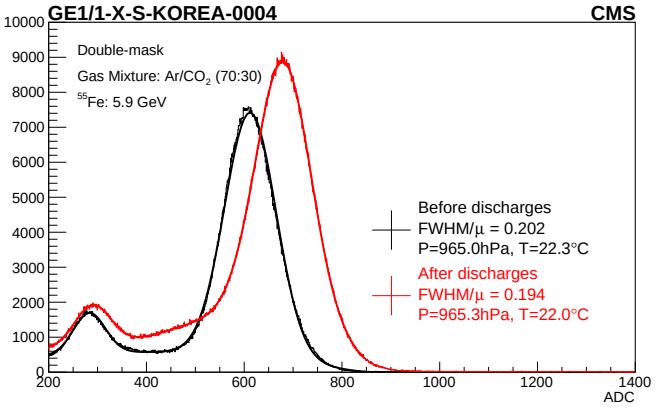

Figure 11: Energy spectra of x-rays from a ^{55}Fe source irradiating a GE1/1 detector with Mecaro foils before and after operation with discharges.

has been modified to increase rate capability [16].

To evaluate the effects of aging, properties of detectors with Korean foils were monitored during exposure to high-flux radiation. The first GE1/1 detector assembled with Korean foils was installed in GIF++ in January, 2018. The initial gain was adjusted to be 2×10^4 and the detector was exposed to 662 keV γ-rays emitted from a 14.1 TBq ^{137}Cs source whose radioactivity was calibrated in 2015. During exposure, I_{ro} was measured to calculate the normalized gas gain and the collected charge. Gain fluctuation from environmental variation was suppressed as described in [19].

Fig. 12 presents the normalized gas gain as a function of charge collected by readout. No degradation of detector performance was observed up to a collected charge of 82 mC cm^{-2} that corresponds to the value expected for GE2/1 detectors after operation for 273 years under HL-LHC conditions.

Because of the much larger accumulated charge expected for ME0 compared to GE1/1 and GE2/1, new measurements are in progress to study aging behavior with much larger fluxes than obtained in 2018. The current measurements utilize an x-ray generator with a Ag transmission target as the radiation source instead of the ^{137}Cs source. Because the interaction cross section of the lower energy x-ray is significantly higher than that of the γ-ray from ^{137}Cs, a faster charge collection rate is achievable even though the intensity of the x-ray generator is lower than that of the ^{137}Cs source [19]. The detector under test is a GE2/1 M7 detector, which is equipped with double-segmented foils. The foil is divided into several sectors, encompassing an area of approximately 10 cm^2, and each sector is electrically isolated through resistive coupling on both the top and bottom sides of the GEM foil. This configuration effectively inhibits the propagation of discharges from one foil to the adjacent foil [20]. In contrast, the GE1/1 detectors use single-segmented foils, which means that only the top side of the GEM foils is segmented.

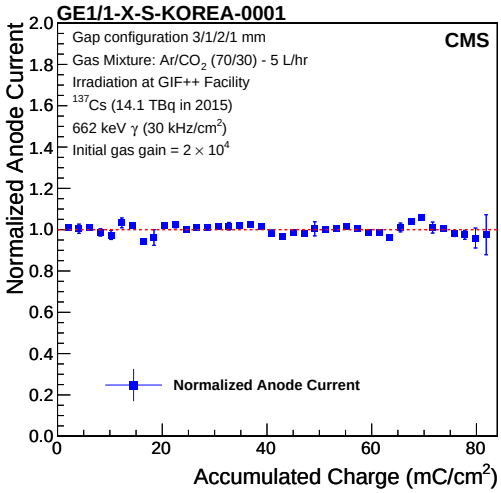

Figure 12: Normalized gas gain as a function of charge collected by readout to test for evidence of aging.

4. Mass production results and plan

The successful completion of QC and QA of GEM foils provided by the new vendor enabled the KCMS collaboration to begin mass production of these foils. From May 2021 to September 2022, KCMS produced GE2/1 foils, of which 292 foils passed the QC criteria and are being used in the assembly of GE2/1 detectors. The 292 foils correspond to 64 % of the number requested to be built by KCMS. Unfortunately, mass production was suspended because the KCMS-Mecaro consortium ended. The production facility is being relocated with completion expected by mid-2023, after which KCMS will start mass production of ME0 foils.

5. Summary

We have validated the performance of GEM foils with an area of approximately 0.6 m^2 produced by a new vendor, the KCMS and Mecaro consortium, employing the double-mask technique for the GE2/1 and ME0 detectors for the Phase-2 upgrade of CMS. After verifying that the dimension and structure of the produced foils were within the designed range, electrical evaluation of the foil's cleanliness was performed based on the QC methodology developed for the CMS upgrade. Subsequently, CMS GE1/1 short-type detectors were assembled with the foils. After the integrity of the assembly was validated, several properties of the detectors were measured. The detectors assembled with Korean foils were comparable in quality to the CERN detectors, and they satisfied the requirements of the CMS upgrade in terms of the effective gain, response

uniformity, rate capability, discharge probability, and robustness to discharges. Evaluation of hardness to classical aging was studied and no degradation of the detector performance was observed up to a charge collection of $82\,\mathrm{mC\,cm^{-2}}$. A new aging study for the ME0 requirement is in progress. The successful QC and QA results enabled the KCMS collaboration to begin mass production of GE2/1 foils. Of these foils, 292 passed the QC criteria and are being used in the assembly of GE2/1 detectors. Since the consortium between the KCMS collaboration and Mecaro has ended, equipment is being transferred to KCMS for mass production of ME0 foils.

Acknowledgments

We thank Dr. Alexander J. G. Lunt (CERN) for taking SEM images of the foils and Dr. Matthew Posik (Temple University) for measuring the uniformity of hole diameters. We gratefully acknowledge financial support from FRS-FNRS (Belgium), FWO-Flanders (Belgium), BSF-MES (Bulgaria), MOST and NSFC (China), BMBF (Germany), CSIR (India), DAE (India), DST (India), UGC (India), INFN (Italy), NRF (Korea), MoSTR (Sri Lanka), DOE (USA), and NSF (USA).

References

[1] F. Sauli, GEM: a new concept for electron amplification in gas detectors, Nucl. Instrum. Methods Phys. Res. A, 386 (1997) 531 - 534, http://www.sciencedirect.com/science/article/pii/S0168900296011722

[2] G. Apollinari, et al., High-luminosity large hadron collider (HL-LHC): Technical Design Report V. 0.1, CERN, Geneva, 2017, http://cds.cern.ch/record/2284929

[3] CMS Collaboration, CMS TDR, CERN-LHCC-2015-0122015, 2015, https://cds.cern.ch/record/2021453

[4] LHC longer term schedule is available at https://lhc-commissioning.web.cern.ch/schedule/LHC-long-term.htm

[5] CMS Collaboration, CMS TDR, CERN-LHCC-2017-012, 2017, https://cds.cern.ch/record/2283189

[6] M. Lamont, LHC accelerator: status and perspectives, plenary talk at ICHEP 2022, Bologna, https://agenda.infn.it/event/28874/contributions/171905/

[7] Mecaro Co. Ltd., Wonnamsandan-ro, Wonnam-myeon, Eumseong-gun, Chungcheongbuk-do, Republic of Korea, 27721, http://www.mecaro.com

[8] S.D. Pinto, et al., Progress on large area GEMs, JINST 4, (2009) 12009, https://doi.org/10.1088%252F1748-0221%252F4%252F12%252Fp12009

[9] I. Yoon, Techniques for mass production of large-sized GEM foil by the Korean CMS group for CMS phase-2 upgrade, JINST 18 (2023) C06010, https://doi.org/10.1088/1748-0221/18/06/C06010

[10] D. Pfeiffer, et al., The radiation field in the gamma irradiation facility GIF++ at CERN, Nucl. Instrum. Methods Phys. Res. A, 866 (2017) 91 - 103, http://www.sciencedirect.com/science/article/pii/S0168900217306113

[11] M. Posik, B. Surrow, Optical and electrical performance of commercially manufactured large GEM foils, Nucl. Instrum. Methods Phys. Res. A, 802 (2015) 10 - 15, http://www.sciencedirect.com/science/article/pii/S0168900215010001

[12] M. Posik, Personal communication, (2017)

[13] D. Abbaneo, et al., Quality control and beam test of GEM detectors for future upgrades of the CMS muon high rate region at the LHC, JINST 10 (2015) C03039, https://doi.org/10.1088%2F1748-0221%2F10%2F03%2Fc03039

[14] R. Venditti, Production and quality control of the new chambers with GEM technology in the CMS muon system, Nucl. Instrum. Methods Phys. Res. A, 936 (2018) 476 - 478, http://www.sciencedirect.com/science/article/pii/S016890021831581X

[15] M.J. French et al., Design and results from the APV25, a deep sub-micron CMOS front-end chip for the CMS tracker, Nucl. Instrum. Methods Phys. Res. A, 466 (2001) 359 - 365, http://www.sciencedirect.com/science/article/pii/S0168900201005897

[16] M. Bianco et al., High rate capability studies of triple-GEM detectors for the ME0 upgrade of the CMS muon spectrometer, JINST 17 (2022) C02009, https://doi.org/10.1088/1748-0221/17/02/c02009

[17] G.J. Feldman, R.D. Cousins, Unified approach to the classical statistical analysis of small signals, Phys. Rev. D, 57 (1998) 3873 - 3889, https://link.aps.org/doi/10.1103/PhysRevD.57.3873

[18] L. Guirl, S. Kane, J. May, J. Miyamoto, I. Shipsey, Nucl. Instrum. Methods Phys. Res. A, 478 (2002) 263-266, https://www.sciencedirect.com/science/article/pii/S0168900201017685

[19] F. Fallavollita, Aging phenomena and discharge probability studies of the triple-GEM detectors for future upgrades of the CMS muon high rate region at the HL-LHC, Nucl. Instrum. Methods Phys. Res. A, 936 (2019) 427 - 429, http://www.sciencedirect.com/science/article/pii/S0168900218314943

[20] J.A. Merlin, Study of discharges and their effects in GEM detectors, talk at MicroPattern Gaseous Detectors Conference, 5-10 May, 2019, La Rochelle, France, https://indico.cern.ch/event/757322/contributions/3396501/